The role of electrostatics in the B to A transition of DNA: from solution to assembly

2007 J. Phys.: Condens. Matter 19 416103

(http://iopscience.iop.org/0953-8984/19/41/416103)

IOP PUBLISHING JOURNAL OF PHYSICS: CONDENSED MATTER

J. Phys.: Condens. Matter **19** (2007) 416103 (19pp) doi:10.1088/0953-8984/19/41/416103

The role of electrostatics in the B to A transition of DNA: from solution to assembly

Laura Rudd, Dominic J Lee and Alexei A Kornyshev

Department of Chemistry, Faculty of Natural Sciences, Imperial College London, SW7 2AZ London, UK

E-mail: dj.lee@imperial.ak.uk

Received 3 April 2007, in final form 12 July 2007
Published 10 September 2007
Online at stacks.iop.org/JPhysCM/19/416103

Abstract

On the basis of a wealth of published experimental data and computer simulations, we build a simple physical model that allows us to rationalize the A to B transition of DNA in solution and in aggregates. In both cases we find that the electrostatic interactions are strong enough, alone, to induce the transition independently of other energetic contributions, e.g. those related to hydration. On the basis of this analysis we conclude that in ethanol/water mixtures, the effect responsible for the transition is the reduction of dielectric constant in the mixture. This is manifested in electrostatic self-energy terms that include the interaction of phosphate charges with condensed counterions. But in dense aggregates, electrostatics plays a dual role, giving rise to two competing effects. In the absence of groove localized counterions the electrostatic self-energy favours the B form, and the electrostatic interaction energy between neighbouring DNA favours the A form. However, the addition of enough counterions localized in the narrow groove reverses this. In dry aggregates of DNA both terms, in most cases, conspire to keep DNA in the A form. The analysis gives a broad picture of the B to A transition and sets a number of new research goals, particularly concerning simulations that may test our simple model for aggregates.

1. Introduction

Right-handed double-helical DNA molecules are known to exist in one of two major structural forms, A and B. Famously, Watson and Crick were first to determine the structure of B-DNA, their findings much later confirmed by the single-crystal x-ray structure of Drew *et al* [1]. This initial discovery was based on fibre diffraction data of Franklin and Gosling [2] and Wilkins and colleagues [3]. The latter collaboration rapidly followed up Watson and Crick's result by the announcement of a new DNA structure, the A-form [4], which has a distinctively different

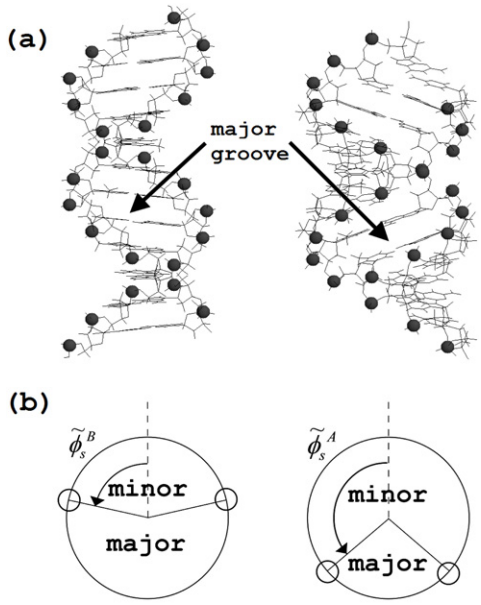

Figure 1. (a) The DNA duplex d(CGCAAATTTCGC) (comprising just over one full helical turn of DNA) in its B-(left) and A-forms (right). Phosphorus atoms are represented as solid spheres to emphasize the locations of the anionic phosphate groups. (b) Cylindrical cross-sections of the canonical versions of the respective forms: values for the angular halfwidths of the minor grooves of B- and A-forms, ϕ_s^B and ϕ_s^A respectively, are given in table 1. The figures illustrate the most important difference between the B- and A-forms from the point of electrostatics: the width of the major groove.

backbone conformation. Under physiological conditions and in laboratory experiments in aqueous electrolyte solution DNA is usually observed in the B-form. But DNA is frequently seen to deviate from this conformation due to changes in its environment related to dehydration, or when bound to proteins. The A- conformation is thought to play an important role in basic genetic processes [5, 6]. For example, during replication the nascent DNA strand at the active centre of DNA polymerase is in the A form. One view is that this results from the dehydration of the duplex by the enzyme and that its biological purpose is to minimize the risk of errors during replication [7], because A-DNA is more structurally conservative than B-DNA [8]. Hence, a thorough grasp of the effects of environment on the A to B transition is likely to be important for a good understanding of DNA's biological function.

The essential difference between A- and B-type structures lies in the puckering modes of the sugars on the sugar–phosphate backbone, C3′-endo for A families and C2′-endo (or the equivalent C3′-exo) for B families. From this disparity arises an important feature; a distance between adjacent phosphates along the same polynucleotide chain of 5.9 Å for the former but 7.0 Å for the latter sugar configuration [8]. For this reason alone, the two types of helix look very different (see figure 1). Structurally, the A-form is energetically disfavoured with respect to the B-form due to the higher internal energy of the C3′-endo ribose sugar conformation. However, by changing the environment in certain ways one may lower the free energy of the A form sufficiently to induce a transition. If one changes the relative humidity (RH) of fibres or films, one may stabilize DNA either in A-form (low RH) or B-form (high RH). Adding some alcohol to the DNA solution also induces the B to A transition [9–11] and excess salt prohibits [9–11] or drives [12] it depending on base-pair content (AT-rich or GC-rich).

This sensitivity of the structure of DNA to humidity, solvent and salt effects has been well established. However, the exact way in which the environment controls the DNA conformation at the molecular level is still not fully understood. The predominant mechanism(s) by which changes in environment drive the transition are still a subject of debate.

The transition widths and mid-points with respect to relative water content of the environment surrounding the molecules are similar in fibres and in isotropic mixed-solvent solution. Because of this, early theories (e.g. [13]) tended to suggest that the B to A transition was primarily driven by differences in hydration free energies due to variations in the mode of binding of water to the two types of DNA. The idea was that under dehydrated conditions the A-form is favoured via hydration free energy as water molecules bind to it more efficiently.

Furthermore, the role of cations in the transition was thought to be limited to their competing with the DNA for water molecules. Their direct electrostatic interactions with the molecule were thought not to be very important. However, in recent years there has been a growing realization that the electrostatic free energy of the system, especially with regard to counterions, may be very important in the modelling of conformational phase transitions of DNA, and may even dominate the impetus for the B–A transition. Within the past decade, simulations of A- and B-DNA in water and water/ethanol mixtures have revealed that the key feature in determining conformational stability of DNA appears to be the free energy due to direct electrostatic interactions between mobile metal ions and phosphate groups across the major groove, and not simply alterations in the hydration shells with changes in relative humidity as was initially supposed [14–18].

In this study, we use a simple approach based on electrostatic potentials that arise from the helical structure of the DNA molecule. We evaluate the electrostatic free energy of the molecule in the presence of counterions, some of which may be groove localized. Throughout the paper, we shall limit ourselves to long strands of native DNA. In section 2 we examine the case of an isolated molecule in a binary ethanol/water mixture. Although the single molecule has been very much studied, we still think this is a useful exercise as a simple model may capture the most important physics of the transition. Indeed, we show how a B to A transition may be induced, as a consequence of electrostatic effects *alone*, by increasing the ethanol concentration.

In section 3, we will move from the isolated molecule in solution to dry aggregates, in which DNA is most commonly observed in the A-form. This is the main emphasis of our paper. Unlike for the single molecule, little theoretical work has been done on the A to B transition in dry assemblies [19], and, in the main, the results we present here are quite new. Since our electrostatic model describes the behaviour of the single molecule well, it seems reasonable that it should also be able to describe some aspects of the behaviour of these assemblies. In such assemblies, the DNA molecules form dense columnar crystal-like structures. As the molecules are close together, we must introduce an important new ingredient into our treatment: electrostatic interactions between DNA molecules within the columnar assembly.

There was substantial progress in a theoretical description and understanding of helix specific effects in the electrostatics of polyelectrolytes and biomolecules [19–22]; for review see [23]. Previous theoretical work [19] *suggested* that the helix specific interaction between a pair of DNA molecules in a dense crystal might provide impetus for the transition as it favours the A-form by >1 kT per base-pair length. Our present work builds on that analysis to treat the entire system. In dry aggregates, the molecule interacts with six nearest neighbours. We will solve the resultant many-body problem. Such a problem has already been studied in hydrated assemblies [22] but this is the first time it has been investigated in dry aggregates. We also include an intramolecular energy contribution. We make certain other improvements: the original analysis [19] was based on a model in which the phosphate strands are described

as infinitely thin helical line charges on the surface of a solid cylinder, while here we give them a finite size.

Based on this study we will be able to conclude that in the aggregate, electrostatic forces between DNA molecules, intimately connected with the helical nature of their charge distributions, are large enough to overcome intrinsic forces that otherwise stabilize the B-form and, independently of other contributions, provide a sufficient driving force for the transition. It was suggested by the authors of [24, 25], based on their experimental work, that this is the reason for the transition in the crystal, but it was not demonstrated by a theoretical study. Our analysis also explains some other features: for example, an interplay between the conformation of the DNA molecules and the lattice structure of the assembly of molecules in such aggregates.

Although our model may lack quantitative reliability in the absence of an atomistic description of the solvent, we think that our results are qualitatively correct as to the nature and scale of the effects that electrostatics has on the conformational structure of DNA. In section 4, we suggest possible simulations that take account of discrete water, to confirm our findings. Many simulations have been done for the single molecule, confirming the crucial role of electrostatics in the B to A transition, but nothing comparable has yet been done for the assembly, and we suggest how this may be achieved.

2. The B–A transition of the single molecule in isotropic, mixed-solvent solution

2.1. Basic model

We shall now construct a simple model for an isolated molecule in mixed-solvent solution based on electrostatic interactions and see how the free energy between the two forms changes with varying alcohol concentration. Here, we assume that the distribution of phosphate charges may be considered as two continuous strands. This assumption is quite reasonable when one accounts for the natural width of the distributions of electronic charge, as well as smearing due to thermal motion. In our treatment of the counterion–counterion interaction we will assume no correlations as interactions between monovalent counterions are relatively weak. We also include the counterion entropy. We will determine the counterion distribution about the molecule self-consistently, subject to some simplifying approximations.

First, we divide up our system as shown in figure 2; a hard-core DNA radius a that is surrounded by an inner layer of solvent of width b (the 'adsorption' layer) and, outside that, an outer, or 'bulk', layer that extends to infinite radius. We take $b = 3$ Å, corresponding approximately to the diameter of a single water molecule.

In the core region, the dielectric constant will be taken as $\varepsilon_c \approx 2$. We'll assume that the dielectric response for charges in the bulk layer is at its macroscopic value. This depends on the percentage of ethanol content of the bulk solution. (Data for dielectric constants of binary mixtures of water and alcohols as a function of composition are taken from [27]). Such data may be fitted to a high accuracy by an empirical equation:

$$\varepsilon(x_v) = 78.46 - 47.96x_v - 9.75x_V^2 + 3.40x_v^3 \qquad \text{at 298 K}, \tag{1}$$

where $0 < x_v < 1$ is the proportion of ethanol in the solution by volume.

For the adsorption layer, the dielectric constant will be taken to be smaller than that of the bulk region. This is due to the very small number of water molecules lying between the closely packed phosphate and counterion charges and the fact that the structure of the water molecules close to the DNA is very much frozen by phosphate charges and steric factors, which limits the dielectric response. Still, allowing for at least single-molecule librations and partial rotations not to be frozen, we will not set $\varepsilon_{ad} \approx 2$. Unfortunately, it is difficult to pin down exactly

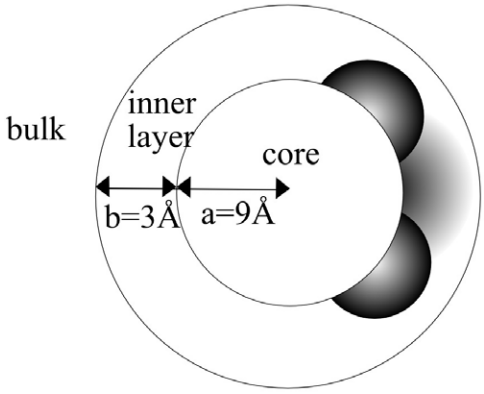

Figure 2. Cross-section of a single molecule with hard-core radius a surrounded by an inner solvent layer of width b and, outside that, an outer, or 'bulk', layer that extends to infinite radius; all fixed charges, i.e. phosphates and ions inhabiting or localized about the grooves, are confined within the inner layer. The charge distribution of counterions in the bulk layer is assumed uniform in the azimuthal sense. The dielectric constants of the bulk and inner layers will be taken to be different.

what the effective dielectric constant inside this layer should be, but judging from the form of empirical dielectric functions used in the literature [28–30] we may reasonably expect it to fall somewhere in the range between 5 and the bulk value of the mixed solvent.

We will model the dielectric constant in the inner layer in the following manner

$$\varepsilon_{\mathrm{ad}} = \gamma + \beta\varepsilon_{\mathrm{B}}, \tag{2}$$

where we have two phenomenological constants, α and β. In principle, we may fix both of them though experiment. If we set $\beta = 0$, we assume that the composition of the layer is essentially independent of the bulk ethanol concentration due to a tightly bound hydration shell. If we fix $\gamma = 0$, the ethanol composition in the adsorption layer is assumed to vary in a similar manner to that of the bulk[1], implying significant ethanol penetration of the adsorption layer.

To calculate the electrostatic free energy of the adsorption layer we need to solve Poisson's equation using the effective dielectric constant for the layer. We will neglect image charge effects due to the boundary between the adsorption layer and bulk. However, we shall include image charge effects arising from the boundary between the low dielectric core and the adsorption layer as these are more significant. In the inner layer we consider, exclusively, charge distributions that are helically symmetric about the molecule. Modelled in this way are phosphate strands and ions that inhabit (or are localized about) the grooves by virtue both of adsorption and of dynamical localization. The phosphates are treated as extended charges that are smeared both in the axial (azimuthal) and radial sense. They have axial and radial Gaussian halfwidths of $w/2$, where $w = 5$ Å. For the phosphate charges the Gaussian peak is centred

[1] This may be reasonable at water–ethanol compositions close to the transition point. Calculations [31] for a uniform cylinder of DNA radius and charge density suggest, for both forms, that at the composition of solution close to the transition point the mixing entropy allows a significant amount of ethanol to penetrate the adsorption layer. These calculations may be overly crude, as they rely on the macroscopic dielectric response and do not take into account the hydration effects due to base pair composition, helical charge patterns and minor groove geometry. Nevertheless, the strength of the effect is striking.

radially at $r = 9$ Å. Azimuthally, the distributions of the counterions are centred in either the narrow groove or the wide groove positions. The fractions of ions in the narrow and wide grooves are given by f_1 and f_2, respectively. Throughout, for simplicity, we shall consider no counterions localized on top of the phosphates. Steric constraints due to hydration mean that ions, on top of the phosphates, should screen out the phosphate–phosphate interactions much less effectively than those in the grooves. Therefore, the effects from such ions may be neglected. The helically symmetric distributions of counterion charge are treated in a similar manner to that of the phosphates but may have a different axial width, which we estimate[2] as $w_c \sim 7$ Å.

For simplicity, in the bulk solution, the distribution of counterions is calculated via the Poisson–Boltzmann equation for a uniformly charged cylinder [33]. One constructs a cylinder of radius R about the molecule in which all counterions lie and, to model the limit of infinitely low concentration of DNA in solution, one takes R to infinity.

We need also consider an internal structural energy, F_{struct}, of the DNA molecule. This may include contributions from internal steric interactions and internal electrostatic self-interactions involving the bases. The A and B conformations correspond to energy minima in F_{struct}. Unfortunately, all-atom structural calculations involving various force fields have so far yielded inconsistent conclusions regarding the energy difference, $F^{\text{A}}_{\text{struct}} - F^{\text{B}}_{\text{struct}}$, and energy barrier between the states [34, 35]. Therefore, we adopt a simpler approach. Our model for the intramolecular energy comprises, simply, the ribose sugar conformational energy and electrostatic interactions between phosphates. The C3′ conformation, corresponding to the A-form, is associated with a potential energy about 1 kcal mol^{-1} ($\sim 1.67 k_{\text{B}}T$ at $\sim$300 K) per monomer (nucleotide pair) greater than that corresponding to the B-form. This has been confirmed (with small variations) via experimental [36] and theoretical [37, 38] studies that treat the ribose sugar or nucleotide as a small, isolated compound.

Important structural parameters that we will employ in our calculations of the free energy of both forms are given in table 1.

From the above considerations, we may calculate the free energy of the single-molecule system (see appendix). We assume the molecule is long enough that its finite length effects may be neglected. Although, generally, we may minimize the free energy with respect to both counterion groove occupancies, f_1 and f_2, we will simplify the problem, assuming that for non-specifically adsorbing ions wide groove sites are less favoured because of phosphate–counterion interactions being less strong. We will therefore simply set $f_2 = 0$ and may then minimize our energy with respect to f_1.

[2] Let's assume, for simplicity, that the counterions lie at the same radial distance away from the molecular axis as the phosphates. Now, if the electronegative regions in within the grooves are taken into account, the electrostatic potential is lowest at the centre of the narrow groove for both B-form (Bartenev *et al* [32]) and A-form (Lipanov *et al* [32]) DNA. Furthermore, ions will attempt to position themselves in the grooves in such a way as to lower their hydration energy, which is achieved best when ions sit at the centre of the groove. Therefore, we might expect the ions to sit as close as possible to the centre of the groove. We will assume that the groove can accommodate at maximum two ions per base pair. The maximum number of ions corresponds to full compensation of a base pair as there is no electrostatic impetus for more ions to sit in the vicinity of that base pair: of course, we have neglected the possibility for overcharging related to correlation effects typical for multiply charged ions (Grosberg *et al* [32]). We represent each ion as a charged sphere surrounded by its first hydration shell. We also give each phosphate group a hydration shell, assumed for simplicity to be the same width as of the counterion. We construct a type of lattice model of sites at which ions can sit on, in the grooves. In the case of B-DNA, the sites of counterion location should lie close as possible to the groove centre and must accommodate the ions' first hydration shells. In the more constricted narrow groove of the A-form, the first hydration shells of the phosphates may overlap with those of the ions. Therefore, we optimize our distribution of sites by minimizing the overlap of all the first hydration shells. We then allow ions to freely move from site to site in a delocalized fashion, neglecting the effects of counterion correlations. The calculations in section 2.2 are actually quite insensitive to the value of w_c when it is within the range $\sim$6–9 Å.

Table 1. (Adapted from [19]): basic helical parameters for A- and B-DNA used in our calculations of electrostatic potential. Here, N is the number of base pairs per helical term (in crystalline state [39] (Note: Although, strictly speaking, it should be noted that the figure of 10 base pairs per turn quoted earlier for crystalline-fibre B-DNA does not exactly persist when it is in solution. Once the lattice breaks down and packing constraints are no longer present, B-DNA unwinds slightly, the new structure having 10.3–10.6 base pairs per turn)), H is the helical pitch, h is the axial rise between phosphate groups on the same backbone, $\tilde{\phi}_s$ is the angular halfwidth of the minor groove and $\tilde{\phi}_n$ is the halfwidth of the *narrow* groove, while w_n is the perpendicular width of the narrow groove. The radius of DNA is practically unchanged and ≈9 Å.

DNA type	N	H (Å)	h(Å)	$\tilde{\phi}_s$ (rad)	$\tilde{\phi}_n$ (rad)	w_n (Å)
A	11	28.2	2.56	0.66π	0.34π	8.5
B	10	33.7	3.37	0.4π	0.4π	11.5

2.2. Incorporation of base-pair specific effects

One sees strong base-pair specific effects when adding alkaline ions to DNA. It is possible for cations to bind directly to base regions deep within the minor groove of B-DNA [40–43]. It is a well known fact that AT-rich sequences are far more resistant to the B to A transition than GC-rich sequences [8]. Cations are able to stabilize AT base pairs more efficiently than GC base pairs and, furthermore, it is found that the strength of binding of ions to the groove of B-form decreases in the order Cs+ > Rb+ > K+ > Na+ [40], following the increase in the binding strengths of the ions to their hydration shells.

To take account of these effects, we may introduce a 'chemisorption' term $E^{\mathrm{B}}_{\mathrm{chem}} = f_1 V$, where V, which is negative and has units of $k_{\mathrm{B}}T$, is the change in energy per ion on entry to the groove. For completely random base-pair sequences we will assume that $V = 0$, for the sake of avoiding the introduction of another adjustable parameter. We do not have a precise value for V but it is reasonable to expect it to fall within the range $-2 < V \leqslant 0$ for other cases.

2.3. Results and discussion

The bulk dielectric constant at the transition mid-point (∼72.5% of ethanol in water [44]). is $\varepsilon_{\mathrm{B}} = 40$ at 298 K (see equation (1)). We solve our model equation (2) for the inner layer dielectric constant as follows: at the transition mid-point we set the energy difference between A and B forms, $\Delta E_{\mathrm{AB}} = E_{\mathrm{A}} - E_{\mathrm{B}}$, to zero. In what follows we will assume that, in equation (2), $\gamma = 0$ and fix β, using the value of the bulk dielectric constant at the transition point. We find that $\beta = 0.29$. We calculate the values of f_1 and the corresponding energy difference ΔE_{AB}. In figure 3, this energy difference and the counterion occupancy are shown as functions of bulk solvent composition.

From figure 3 we see that the energy difference ΔE_{AB} decreases monotonically with increasing ethanol concentration about the point where $\Delta E_{\mathrm{AB}} = 0$ (the transition point). The counterion fraction stays roughly the same with composition and is higher for the A-form than for the B form ($f_1 \approx 0.5$ and 0.25 respectively) because its two phosphate strands are much closer together, which provides a greater incentive for counterions to localize about the narrow groove. Three factors limit the size of f_1: (i) interion repulsions, (ii) entropy in the adsorption layer which does not favour too large a large value of f_1, and (iii) bulk solution free energy, which does not allow the effective compensation to exceed the Manning value.

Now let's examine why we get the correct qualitative behaviour for ΔE_{AB} as a function of volume fraction of ethanol. Let us consider a simple model of parallel line charges long enough to be considered effectively infinite. Two one-dimensional negatively charged strands of linear

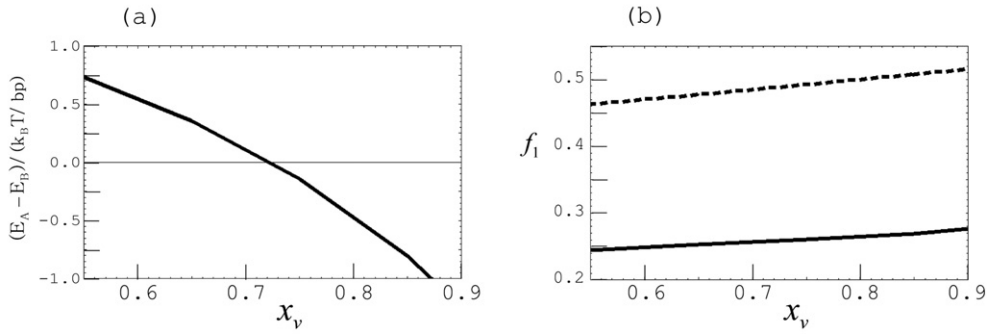

Figure 3. (a) Energy difference between A and B forms, $\Delta E_{AB}/(k_B T$ per base pair) against x_v, the fraction of ethanol by volume of the bulk solution. (b) Optimized value of the fraction, f_1, of counterions in the narrow groove against x_v; solid = B-form, dotted = A-form.

charge density[3] $-\lambda/2$ are separated by the perpendicular distance that represents the widths of either of the two grooves, w_A and w_B (see table 1), while a parallel positively charged strand of linear charge density $+f\lambda$, where $0 \leqslant f \leqslant 1$, is centred at their mid-point. For such a model we find the following difference in the electrostatic energy, $E_A^{\text{line}} - E_B^{\text{line}}$:

$$E_A^{\text{line}} - E_B^{\text{line}} = \frac{2L\lambda^2}{\varepsilon_{\text{ad}}}\left\{\frac{1}{4} - f\right\}\ln\left(\frac{w_B}{w_A}\right). \tag{3}$$

As $w_B > w_A$, $E_A^{\text{line}} - E_B^{\text{line}}$ is positive if $f = 0$, i.e. if there is no positive charge in the groove. Thus the B form is favoured if $f = 0$. However, if the positive counterion fraction surpasses $f = 0.25$, the energy difference reverses in sign and the electrostatic energy favours the A-form.

The double helix has a more complicated geometry than the simple system just presented but the principle behind the transition is the same. Once the critical ion fraction has been surpassed, a reduction in the local dielectric constant, ε_{ad}, increases the difference between the electrostatic potential energies of the A and B forms in favour of A form. In addition, at equilibrium the A-form tends to have a higher value of f_1 than does the B form, which provides more electrostatic impetus for the transition.

We find that our model yields a energy difference per base pair of $\Delta E_{AB} \approx 2.8 k_B T$ in pure water ($\varepsilon_B \approx 80$). The authors of [10] estimated a difference of $\sim 1.67 k_B$ T ($\sim$1 kcal mol^{-1}) per base pair between A- and B-forms of DNA in pure water. That estimate was based on experimental study of transition mid-points under varying conditions. The value obtained from our calculations is of the correct order; perhaps slightly too large. However, if we set $\beta = 0$ and fix γ, we find that $\Delta E_{AB} \sim 0.4 k_B T$, which is too small. This implies that the model with $\gamma = 0$ is better, suggesting that a significant amount of ethanol penetrates into the adsorption layer. This seems to be in agreement with the findings of simulations [15, 45].

Now, let us examine the effects of base pair and/or counterion specificity. Our chemisorption parameter V may become more negative as the proportion of AT base pairs increases, or it may vary with counterion species. In figure 4 we plot against $-V$ the transition mid-point (a) and the B-form narrow groove fraction (b). As can be seen, a modest change

[3] The difference between the widths of the grooves of the two forms is more pronounced than that between the linear charge densities of both forms (separations of phosphates along the strands being quoted in [45] as 5.9 and 7.0 Å respectively). Therefore, for the purposes of discussion we will examine the case where the linear charge densities are the same.

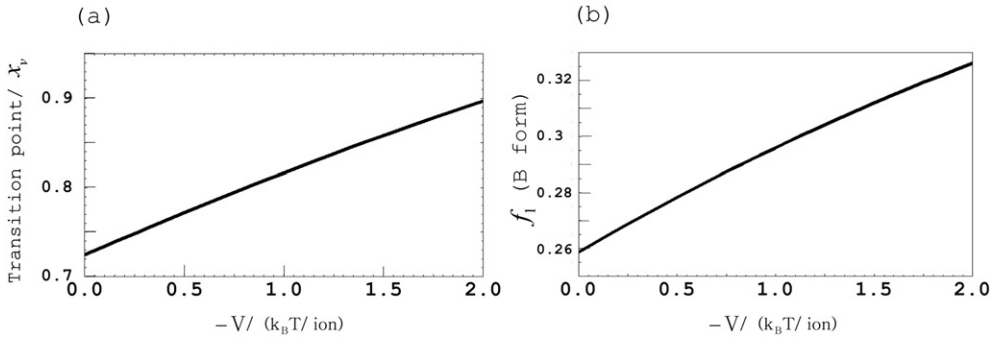

Figure 4. Effect of adding a 'chemisorption' term fV, a favourable energy change per ion in the groove due to electronegative base sites, to the free energy of B form but *not* A form. We use the formula for the dielectric constant of the inner layer, $\varepsilon_{\rm ad}$, that we solved for above, i.e. we use $\alpha = 0$ and $\beta = 0.29$ in equation (2): (a) the transition point, in fraction of ethanol (v/v), x_v plotted against the magnitude of V, which is negative; (b) the narrow groove fraction of ions for the B form (at the transition point) against $|V|$.

in $-V$ changes the ion fraction little but creates a large shift in the transition mid-point. This might describe the trend observed when the species of ion is changed: the ability to shift the transition point to higher fractions of ethanol is different for different ions [10, 11] and the trend appears to correlate with each species' binding affinity to the groove (i.e. magnitude of V). We may interpret the difference in f_1 at finite V from that at $V = 0$ as a fraction of ions that are localized deep within the minor groove, where they interact strongly with the bases. This excess in the counterion occupancy is small: $\Delta f_1 \sim 0.06$, which is consistent with the observations of [14].

As it rationalizes some already known results, this analysis indicates that electrostatics has an important role to play in the B to A transition.

3. The B–A transition in dense aggregates

3.1. Model

In dry aggregates we must consider two electrostatic components in addition to the energy difference between the two sugar conformations. The first is an electrostatic self-energy contribution, considered in the previous section, for the charge distributions associated with each molecule. The second is an intermolecular interaction term that we will discuss later. In dense, dry assemblies it is natural to assume a uniform dielectric constant of $\varepsilon_r \simeq 2$ [19] because in the densest DNA aggregates ions and water molecules are likely to be frozen, either sterically or via strong interactions with the DNA surface. We will also assume that counterion entropy is unimportant.

As before, counterion distributions are centred in either the narrow groove or the wide groove positions (f_1 and f_2 respectively) with the same estimated axial width $w_c \sim 7$ Å. We also introduce a completely non-localized, or 'smeared', counterion fraction f_3, where $f_1 + f_2 + f_3 = 1$ (as the aggregate is electroneutral), spread as an even background everywhere throughout the medium but the cores of the molecules. As we have no theory that predicts the equilibrium distribution of counterions within an assembly, we leave f_1 and f_2 as adjustable parameters and explore the qualitative effects of changing them.

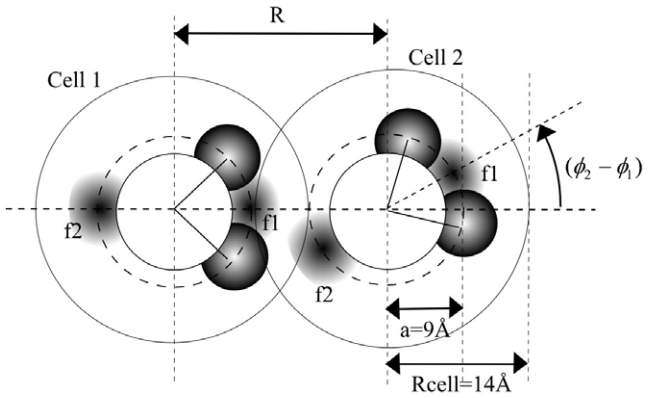

Figure 5. In each cell, the phosphates are treated as objects that are smeared similarly in the axial and radial sense, with a Gaussian width of w. Localized counterions are treated similarly but may have a different width, w_e, than do the phosphates. They are located in either the f_1 ('narrow groove') or f_2 ('wide groove') positions. No counterions are located *on* the phosphates. We may also allow for a completely non-localized, or 'smeared', counterion fraction $f_3 = 1 - f_1 - f_2$. ϕ_i is the azimuthal angle that the middle of the narrow groove of molecule i makes with the line connecting the centres of the two molecule; thus $(\phi_2 - \phi_1)$ is the molecules' relative azimuthal orientation.

For this investigation we will take advantage of the simplicity of a uniform dielectric constant to improve the model of charge distributions. The charged helices are modelled in the same way as described in section 3 but the limits for the radial smearing are altered: the phosphate and counterion[4] charge distributions have Gaussian radial distributions with a peak at $r = 9$ Å but they are cut off at $r = 7.4$ Å (where they should come into contact with their own sugar groups [47]) and at the core of the nearest adjacent molecule.

We define the volume of a cell as shown in figure 5. Here, the molecule lies at the central axis of the cell. All components of the charge distribution that are helically symmetric about the molecule are included in the calculation of the electrostatic self-energy for that molecule. To calculate the self-energy we use Poisson's equation.

The pairwise interaction energy is the electrostatic energy of interaction of the charge distribution associated with one cell with another (see figure 5). Again, to calculate it, we solve Poisson's equation. The interaction energy, E_{int}, between two helical charge distributions of length L can, to a good approximation, be given by the expression [19]:

$$E_{\text{int}} = L[a_0 - a_1 \cos(\phi_1 - \phi_2) + a_2 \cos(2(\phi_1 - \phi_2))]. \tag{4}$$

Here, $\phi_1 - \phi_2$ is defined as the *relative azimuthal orientation* of the two molecules. The azimuthal angle ϕ_i may be defined as the angle that the middle of the narrow groove of molecule i makes with the line connecting the centres of the two molecules in the plane cutting their cylindrical cross-sections. Expressions for the a_n coefficients, which depend on a number of factors such as the charge distribution on the DNA and the dielectric properties of the medium,

[4] Of course, in reality the counterions, which interact with the bases in the grooves, have centres that are not positioned at the same distance from the axis as the phosphates. Generally, we lack detailed information on this. But, there is one case for which we do: the authors of [46] recorded the positions of Cs+ ions in the A-Cs-DNA lattice at 75% r.h. From this we determine the values $\{f_1 = 0.36,\ f_2 = 0.27,\ f_3 = 0.36\}$ as well as the average distance of each fraction from the helical axis. The authors also recorded the positions of Cs+ ions in glucosylated Phage T2 B-DNA [46] at the same humidity: $\{f_1 = 0.5,\ f_2 = 0.5,\ f_3 = 0.0\}$. Unfortunately the latter structure is of limited use to us as this conformation is artificially stabilized and the lattice is at a considerably higher density than the non-glucosylated system. However, such a revised positioning of ion fractions, in this case, still favours the A-form configuration over that of B form.

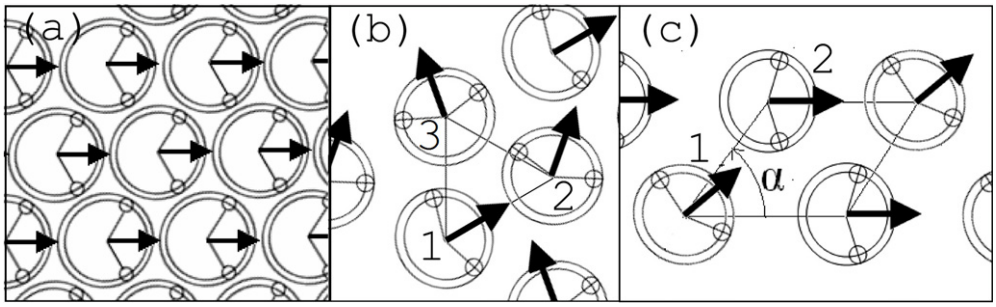

Figure 6. Permitted lattice 'spin' configurations: (a) 'Ferromagnetic', (b) 'Potts' (one of two degenerate arrangements [22] is shown) and (c) 'Rhombic AFI'. See text for details. Large circles are cross-sections of the DNA molecule in the columnar lattice with the small circles representing phosphates. Arrows indicate the middles of the narrow grooves.

may be found in [19] for dry lattices, or in [20, 21] for aqueous assemblies where screening by electrolyte occurs.

The a_1 and a_2 coefficients decay exponentially with increasing interaxial separation, for fixed dielectric constant and counterion distributions of the helices, with characteristic inverse decay lengths $\frac{2\pi}{H}$ and $\frac{4\pi}{H}$ respectively. Therefore for increasing separation, the a_1/a_2 ratio increases. When the a_1 term dominates over the a_2 term, the ground state energy of a pair of molecules is minimized when the two helices have the same value of ϕ_i, i.e. $\phi_1 - \phi_2 = 0$. But at separations below the 'frustration point', the point at which $a_1 = 4a_2$, the energy is minimized at an optimum alignment $\phi_1 - \phi_2 = \phi^*$, where $\phi^* = \cos^{-1}(a_1/(4a_2))$. In a high density columnar lattice this results in particular patterns of relative azimuthal orientations of molecules and possibly lattice distortions in order to optimize the electrostatic energy. These can be fully analysed by solving the many-body problem, briefly reviewed below and discussed in detail in [48].

Many-body calculations suggest three main candidates for the ground state lattice in aggregates in which there is, at least, 2D order [48]. One candidate is the Potts state (see figure 6(b)). Here, the 2D positional structure of the lattice is hexagonal. Around a triangular plaquette as shown, where the vertices are labelled 1, 2 and 3, we have the relative azimuthal orientations of $\phi_1 - \phi_2 = \psi_P$, $\phi_2 - \phi_3 = \psi_P$ and $\phi_1 - \phi_3 = 2\psi_P$ where $\psi_P = 1/4(1 + \sqrt{1 + 2a_1/a_2})$. These then form a repeating structure. However, in such frustrated systems one may also have rhombic positional order. Here, the azimuthal orientations of the molecules (spins) are in an 'antiferromagnetic' configuration (see figure 6(c)). For such a configuration we may label the rhombic unit cell with labels 1 and 2, which signify different spins, in optimum alignment with each other. We minimize the total interaction energy of the lattice with respect to the rhombic lattice angle, α.

Finite temperature can give rise to azimuthal thermal fluctuations [22] which affect the free energy. However, in this study such effects need not be considered as the interaction energies are such that $E_{\text{int}} \gg k_{\text{B}}T$.

3.2. Results and discussion

Using the results of this model we would like to rationalize some experimentally observed trends seen in regard to the B to A transition. The first is that the A-form is favoured in aggregates under very dehydrated conditions. We will use our model to compare A- and B-forms at a lattice density corresponding to a relative humidity (RH) of about 75%. At this and

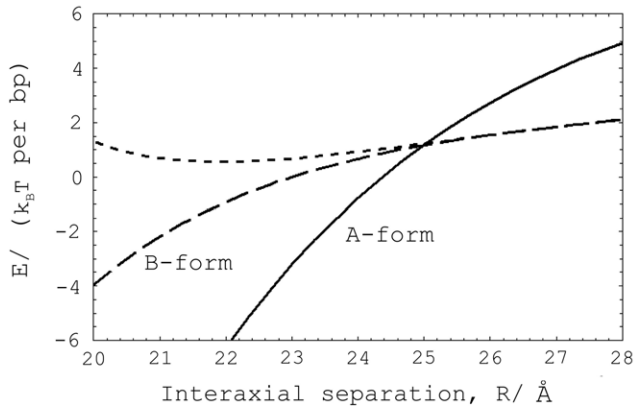

Figure 7. Electrostatic energy, E, in k_BT base pair, in a dense, dehydrated columnar lattice for the case in which compensating counterions are 'smeared' homogeneously throughout the interspatial regions, i.e. $f_1 = f_2 = 0$, $f_3 = 1$. Solid—A-form, ferromagnetic; dashed—B-form, Potts; dotted—B-form, ferromagnetic. The energy is arbitrarily zeroed at the value corresponding to that of the B form for an interaxial separation of 23 Å.

lower relative humidities, Na-, K-, Rb- and Cs-DNA exist in the A-form (although Li-DNA exists in the B-form: this anomaly will be considered later). A mean interaxial separation of 23 Å, which should allow about one water molecule to rest in the space between helices, is a reasonable approximation for both A- and B-forms at this humidity [49, 50].

Assuming a smeared charge distribution of counterions and keeping the dielectric constant fixed at $\varepsilon_r = 2$, as we decrease the interaxial separation the interaction energy between helices strengthens so that the difference in energy per base pair between the B-form and the A-form, ΔE_{AB}, shifts to favour A-form. The results of such a calculation are shown in figure 7. Here, we have plotted the lowest energy state of each conformation: for the A-form, the ferromagnetic state and for the B-form the frustrated Potts state (which is virtually equal in energy to the antiferromagnetic state). We do not consider interaxial separations below 23 Å because under those circumstances steric hindrances, due to the phosphate ridges, will have an important role to play. We see from our results that, at the separations seen in dry aggregates ($R = 23$ Å), the A-form is favoured. Therefore the intermolecular interaction energy *alone* is sufficient to stabilize the A-form.

However, the results of figure 7 should be treated with care. Indeed, first of all the dielectric constant should increase with decreasing aggregate density. Secondly, the balance of entropy and electrostatic interactions causes some of the counterions to 'melt' to form a Debye screening atmosphere, spread out from the helix, whereas others form a 'non-linear' adsorption layer [23]. Both of these effects will diminish the absolute values of ΔE_{AB}. Therefore, figure 7 should be taken as only a qualitative picture of what happens when one changes the separation between molecules. Nevertheless, because of such considerations, the separation at which the transition occurs, $R = 25$ Å, can probably be regarded as an upper estimate.

The fact that the A-form is in the ferromagnetic state while the B-form is in one of the frustrated states has its origin in the difference in groove widths of the two forms and its effect on electrostatic interactions. Because of the A-form's narrower narrow groove the a_1/a_2 ratio is greater for A-form than for B-form. As discussed in the previous subsection it is the relative size of the a_2 term that determines the degree of frustration in the ground state. This is why the B-form lattice is in an azimuthally frustrated state and the A-form lattice is not.

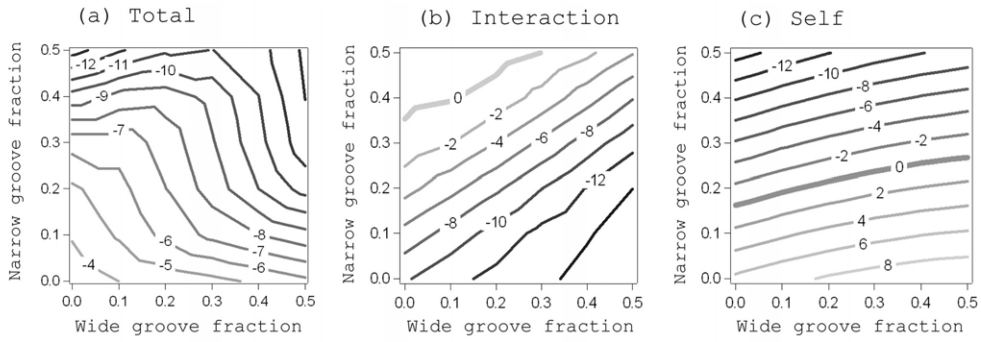

Figure 8. Effect of groove localized counterions on system energy. (a) The energy difference between A- and B-form in k_BT per base pair, ΔE_{AB}, in a lattice with interaxial separation 23 Å, is plotted as a function of the fractions of ions in the narrow and wide grooves. Thus if $\Delta E_{AB} < 0$, A-form is stabilized, otherwise B-form is favoured. The two components of the electrostatic energy difference have also been examined separately: (b) the interaction energy between the 'cells' and (c) the self-energy of each 'cell' (see text). The non-electrostatic contribution due to the sugar molecules is included in the self-energy component.

Now, we shall explore the consequences of allowing counterions to localize in the grooves and how this affects the results. Figure 8 shows the difference, ΔE_{AB}, between the total energies per base pair of A- and B-form DNA for the general counterion distribution $\{f_1, f_2, f_3\}$ (notation explained in subsection 3.1). Throughout, the lattice is hexagonal with parameter 23 Å.[5] We find that the A-form tends to remain in the ferromagnetic state and the B-form (except for the unrealistic, extreme case of large amounts of counterion in the major groove) in the Potts state.

The contributions from the two energy components, self-energy and interaction energy, are presented separately in parts (b) and (c) of figure 8, respectively. The self-energy comprises both the self-electrostatic energy, which is defined in subsection 3.1, and the non-electrostatic intramolecular energy component discussed in section 2.

The two components of ΔE_{AB} are affected differently by changes in counterion distribution. As we increase the narrow groove counterion occupancy and keep the wide groove occupancy fixed, the self-energy of the A-form is lowered (made more favourable) with respect to that of the B-form (see figure 8(c)). This is because the A-form is able to benefit more from phosphate ion attractions due to its narrower narrow groove and denser clustering of phosphates. However (as discussed in [19]), this has precisely the opposite effect on the interaction energy: increasing the occupancy of ions in the narrow grooves favours the B form. On the other hand, increasing the wide groove occupancy increases, rather than decreases, the degree of charge separation on the helix and so causes the interaction energy to favour the A form.

[5] We chose a purely hexagonal arrangement for the following reasons. At 75% RH, the recorded lattice forms for A-DNA (Fuller *et al* [51]) and B-LiDNA (Langridge *et al* [51]) are both very nearly hexagonal (<65° rhombic distortion angle). Although, in the case of the B form, an rhombic antiferromagnetic state could be suggested as possible candidate, it is difficult to work with it here. Indeed, at given relative humidity and therefore fixed lattice density, rhombic distortion will bring some of the helices closer together than is the case for the hexagonal lattice of the same density. We do not have a model for the short range steric (forces) but we know that they should reduce the amount of distortion. Therefore, it makes sense that the lattice should be nearly hexagonal. The Potts state is easer to handle due to no steric constraints at these densities and, in effect, its energy difference from the hexagonal antiferromagnetic state is very slight.

Table 2. Experimentally observed effects of different counterions on properties of A-DNA strands and assemblies. In all cases the trend shown in the third column is a continuous one down Group I, although Li+ is left out as it does not stabilize the A-form in the crystal [8, 11].

Trend	Action of alkali counterion	Strength of the ion effect
I [11]	Stabilizes A-form duplex against melting	Cs+ > K+ > Na+
II [11, 52]	Strengthens the intermolecular interactions between A-form duplexes in the lattice	Na+ > K+ > Cs+

These findings seem to support the conclusions of the authors of [24, 25]. A series of pioneering experimental investigations led them to the conclusion that intermolecular interactions are indeed essential, here. In particular, it was thought that the groove shapes and azimuthal alignment of the A-form duplexes are responsible for the fact that their interhelical forces are stronger than those of the B form and hence for the transition. However, they did not state the exact mechanism by which this occurs, nor provide any estimates of energy difference between the two forms.

Other important results from such experimental work concern the way in which changing the counterion species affects the strength of the interhelical forces. We will show that this can also be rationalized in the context of our model. While all group I counterions from Cs+ to Na+ permit the B to A transition in the solid crystal, a wealth of experimental evidence reveals differences in the effects of the different ion species on measurable properties of the A-form assembly.

Table 2 demonstrates two opposing trends. Addition of alkaline ions to the A-form stabilizes the helix against melting [11]. Here, caesium ions seem to be the most effective and, moving up the alkali metal group of the periodic table, sodium ions the least effective in stabilizing the double helix. On the other hand, the trend in the strength of intermolecular forces, with species of counterion, goes in precisely the opposite direction. This has been deduced by comparing their ability to promote the aggregation of A-DNA in ethanol [11] and by measuring, via speed of sound [52], the strength of the forces between A-DNA molecules in the dry aggregate.

We suggest that the common cause of the two opposing trends is as follows. Large hydration shells do not allow ions to accumulate in large concentrations in the restricted space of the A-form narrow groove[6], so more strongly hydrated ions, such as Na+, tend to screen the phosphates of the narrow groove less effectively than more weakly hydrated ions, such as Cs+. In the aggregate, a decrease in the narrow groove counterion concentration necessarily implies an increase in the concentration of counterions in between the molecules and/or in their wide grooves [54]. Now, in our model, this translates to a reduction in f_1 and/or an increase in f_2 and/or f_3. The result is that phosphate–counterion interactions *weaken*, but intermolecular interactions *strengthen*. So (providing that we are correct in linking a decrease in melting

[6] The idea of steric conflict between groove and ion is not without precedent: the authors of [53] rationalized the A–A′ transition in mixed-solvent solution, seen for Na+ but not for ions that are less hydrated, by the idea of a clash between the size of the hydrated ion and the dimensions of the narrow groove of ordinary A-form (A′-form being a variant with a significantly wider narrow groove). Effects of different ions on a collection of intra-B-family nucleic acid transitions were also rationalized via the same principle.

temperature (trend I) with a rise in self-energy[7]), we can rationalize the two opposing trends discussed above.

This might also explain why some species of counterion, e.g. Li+ and Mg^{2+}, do not favour the A-form in the dry aggregate. What these ions have in common is a very tightly bound hydration shell. While this severely restricts the volume available to them in the narrow groove of A-form, they can be accommodated comfortably in the B-form's spacious minor groove. Calculations [31] consistent with this discussion suggest that it is indeed possible for this effect to energetically destabilize the A-form with respect to the B-form[8].

4. Concluding remarks

To describe the B to A transition in isotropic, mixed-solvent solution, we used a simple calculation of the free energy of the macroion–counterion system. This simple theory does quite well in explaining the transition with variation of the ethanol concentration. The aim of this first exercise was to show that our model conforms with the consensus of simulation authors [14–18] on the electrostatic origin of this transition. It then seems logical that our model should also have some success in describing the behaviour of dry aggregates of DNA in regard to the B to A transition.

Indeed, our model completely supports the suggestion of the authors of [24, 25] that the B to A transition in the dehydrated aggregate is caused by DNA–DNA interactions in crystal packing. Following from [19] (where this driving force was qualitatively analysed for two molecules), using a more complete calculation (intramolecular interactions extended charge distributions etc.) we demonstrate that this effect may, indeed, be the cause of the transition. The low dielectric constant found in the crystal environment is crucial in strengthening electrostatic interactions sufficiently to drive the transition. Furthermore, we find that this phenomenon is indeed intimately connected with both the physical structure and the nature of the packing of the A-form helices, as the authors of [24, 25] advocated. An important issue is the question of why different counterions cause the strength of the interhelical forces to differ. We offer an explanation for it via our model by considering the way in which different ions are likely to arrange themselves around the double helix. Last of all, we speculate, based on steric considerations, why strongly hydrated ions like Li^+ do not favour the A-form in dry aggregates.

We have made several predictions, which we hope atomistic simulations and more sophisticated models will be able to test. Unfortunately, an ingredient missing from the calculations in dry aggregates is a self-consistent determination of the counterion distribution. In further theoretical work, we hope to perform calculations that take into account the statistical mechanics of counterion adsorption in aggregates. Again, an improved treatment of the dielectric response will be important in future work. At the moment, we do not know how well the assumption of a uniform dielectric constant $\varepsilon \approx 2$ works in dry aggregates, nor do we know how a changing dielectric response effects ΔE_{AB} as we increase humidity and separation between molecules.

Besides this, further computer simulations would be useful. Very probably, quantitatively accurate results may only be achieved by an atomistic description of the discrete solvent.

[7] The authors of [54] express a similar opinion to ours on the origin of trend I. On the other hand, they suggest a slightly different rationalization to ours of trend II, i.e. why interhelical forces might be stronger for Na+ than for Cs+. They suggest that ions are positioned so to bridge phosphate groups on two adjacent molecules: however, no quantitative estimate of this effect was given.

[8] We must be careful as this may not be the full story. It is a commonly held view that Li+ has a strong affinity for the minor groove of B-DNA which will influence the stabilization of the B-form. Unlike the other Group I ions, Li^+ ions in the narrow groove may form water bridges with the phosphates [54].

Simulations of the single molecule only began to yield useful results concerning the B to A transition in the last decade and it is hoped that, computational expense allowing, this may prove a real possibility for the aggregate as well. First and foremost, simulations will provide a useful test of whether interactions between neighbouring DNA *are* sufficiently strong to induce the transition. Secondly, our explanation as to why different counterion species cause the interhelical force to differ in strength could also be tested.

A first step would be a 'ground state' simulation. Such simulations should, if possible, contain several DNA molecules arranged in a unit cell. They should be free to find their optimum relative azimuthal orientations. To start with, the positions of certain species of counterions could be retrieved from crystallography, for instance for caesium [40, 56]. Such calculations should work well for dry fibres, where the water is more or less frozen and fluctuations are likely to be small.

As we hydrate the assembly, fluctuations of water molecules and counterions will become more important so that one may be forced to perform molecular dynamics (MD) simulations. Such simulations of counterions, water and DNA are likely to be computationally expensive. However, some MD simulations have already been done in a crystal environment [57] to model how the presence of neighbouring duplexes might affect details of the three-dimensional structure of B-DNA in the crystal, environment. Thus simulations, with an analysis of the various free energy contributions, may provide a starting point for the testing of our predictions.

The main conclusion of this paper is that helix specific electrostatic interactions in assemblies provide a large enough energy contribution to drive the B to A transition independently of other effects.

Acknowledgments

We would like to thank Dr C W Monroe for useful discussions. Financial support from the EPSRC (GR/S31068/01) is also gratefully acknowledged. AAK would also like to acknowledge support from his Royal Society Wolfson Merit Award.

Appendix. Free energy for the isolated molecule

The free energy of the isolated molecule is given by:

$$F = F_{\text{struct}} + F_{\text{env}} \quad = F^{\text{ne}}_{\text{struct}} + F_{\text{ad}} + F_{\text{PB}} - F_0 \tag{A.1}$$

where $F^{\text{ne}}_{\text{struct}}$ is the non-electrostatic structural contribution to the energy difference between A and B forms. F_0 stands for an infinite constant that originates from the extension of the cylindrical cell radius to infinity[9]. The term F_{ad} is the free energy of the inner, or adsorption, layer, given by:

$$F_{\text{ad}} = \tfrac{1}{2}\int_{\text{A}} \mathrm{d}^3 r[-\rho_{\text{phos}}(\mathbf{r}) + \rho^{\text{A}}_{\text{c}}(\mathbf{r})]\phi(\mathbf{r}) + k_{\text{B}}T\sum_{i=1}^{2}\frac{f_i L}{l_{\text{c}}}\left\{\ln\left(\frac{c_{\text{ad},i}}{c_{\max}}\right) + \left(\frac{c_{\text{ad},i}}{c_{\max}} - 1\right)\ln\left(1 - \frac{c_{\text{ad},i}}{c_{\max}}\right)\right\}. \tag{A.2}$$

[9] F_0 diverges with infinite cell radius as $\ln(R_{\text{cell}})|_{R_{\text{cell}}\to\infty}$. It represents the interaction between the partially compensated polyelectrolyte molecule and counterions infinitely far away from it. The problem of the divergence of the potential around an infinite line charge or cylinder at infinite radius is well known and this otherwise problematic feature has been rationalized [58]. Eventually the infinite length approximation will break down when the length of the cylinder becomes small with respect to the radial displacement. Since there will be no difference between the values of this term for A and B forms, we need not consider it further.

Here, $\rho_{\rm phos}(\mathbf{r})$ is the charge density due to the phosphates and $\rho_{\rm c}^{\rm A}(\mathbf{r})$ that due to the counterions within this layer, $\phi(\mathbf{r})$ is the electrostatic potential, $c_{{\rm ad},i}$ is the number density of the counterions within a particular groove and $c_{\max} = (4\pi r_0^3/3)^{-1}$, where r_0 is the hard-core radius of a counterion, is the maximum possible value of this quantity. $l_{\rm c}$ is the length of the DNA molecule that each phosphate unit charge occupies, L is the total length the DNA molecule. The first term in $F_{\rm ad}$ is the electrostatic contribution, which includes phosphate–phosphate interactions, counterion–phosphate interactions and counterion–counterion interactions. Here, the volume integral in the electrostatic term of equation (A.2) extends over the whole adsorption layer and so is proportional to L. Such a term contains helical charge distributions, for which the characteristic length is the DNA helical pitch, H. The assumption of helical ideality is valid provided that $\lambda_{\rm c} \gg H$; here $\lambda_{\rm c}$ is the helical persistence length, which characterizes the non-ideality of the helix (for further discussion of it see [23, 59]). For DNA this condition is easily satisfied. The second term in $F_{\rm ad}$ is the counterion entropy for sites within the groove.

Now, $F_{\rm PB}$ is the free energy of the bulk, given by:

$$F_{\rm PB} = -k_{\rm B}TL\left\{\frac{2\varepsilon_{\rm B}}{\varepsilon_{\rm ad}l_{\rm B}}\ln(\xi_{\rm eff}-1) + \frac{1}{l_{\rm c}}(1-f_1-f_2)\left[\ln\left(\frac{c_{\max}}{c^*}\right)+2\right]\right\} \tag{A.3}$$

where $l_{\rm B} = e^2/\varepsilon_{\rm ad}k_{\rm B}T$, is the Bjerrum length at dielectric constant $\varepsilon_{\rm ad}$. c^* is the number density of the counterions just outside the boundary with the inner layer and takes the form:

$$c^* = \frac{1}{2\pi}\frac{\varepsilon_{\rm B}(1-\xi_{\rm eff})^2}{\varepsilon_{\rm ad}l_{\rm B}}\frac{1}{(a+b)^2}. \tag{A.4}$$

Again, the maximum possible value of the number density is given by $c_{\max}$. In the bulk region, differences in dielectric constant and charge compensation in the adsorption layer give an effective value of the Manning parameter:

$$\xi_{\rm eff} = \frac{\varepsilon_{\rm ad}}{\varepsilon_{\rm B}}(1-f_1-f_2)\xi_{\rm bare}(\varepsilon_{\rm ad}) \tag{A.5}$$

where the bare Manning parameter $\xi_{\rm bare}$ is given [33] by $\xi_{\rm bare} = l_{\rm B}/l_{\rm c}$.[10]

References

[1] Drew H R, Wing R M and Takano T 1981 *Proc. Natl Acad. Sci.* **78** 2179
Dickerson R E and Drew H R 1981 *J. Mol. Biol.* **149** 761
Drew H R and Dickerson R E 1981 *J. Mol. Biol.* **151** 535
[2] Franklin R E and Gosling R G 1953 *Nature* **171** 740
[3] Wilkins M H F, Stokes A R and Wilson H R 1953 *Nature* **171** 738
[4] Franklin R E and Gosling R G 1953 *Acta Crystallogr.* **6** 673
[5] Olson W K and Zhurkin V B 2001 *Curr. Opin. Struct. Biol.* **10** 286
[6] Tolstorukov M Y, Ivanov V I, Malenkov G G, Jernigan R L and Zhurkin V B 2001 *Biophysical J.* **81** 3409
[7] Timsit Y 1999 *J. Mol. Biol.* **293** 835
[8] Saenger W 1984 *Principles of Nucleic Acid Structure* (New York: Springer)
[9] Ivanov V I, Minchenkova L E, Scholkina A K and Poletayev A I 1973 *Biopolymers* **12** 89
[10] Ivanov V I, Minchenkova L E, Minyat E E, Frank-Kamenetskii M D and Schyolkina A K 1974 *J. Mol. Biol.* **87** 817
[11] Rupprecht A, Piskur J, Schultz J, Nordenskiold L, Song Z Y and Lahajnar G 1994 *Biopolymers* **34** 897

[10] The effective Manning parameter may not fall below 1, as the free energy becomes very large and positive. Physically, in the absence of the counterion correlations, one cannot compensate the charge of the DNA in the adsorption layer above the Manning fraction $\theta_{\rm M} = 1 - 1/\xi_{\rm eff}$; due to entropic effects the fraction of the counterions $(1-\theta_{\rm M})$ drift out into the bulk solution and are no longer localized about the molecule [60].

[12] Nishimura Y, Torigoe C and Tsuboi M 1986 *Nucleic Acids Res.* **14** 2737
[13] Saenger W, Hunter W N and Kennard O 1986 *Nature* **324** 385–8
[14] McConnell K J and Beveridge D L 2000 *J. Mol. Biol.* **304** 803–20
[15] Sprous D, Young M A and Beveridge D L 1998 *J. Phys. Chem.* B **102** 4658
[16] Jayaram B, Sprous D, Young M A and Beveridge D L 1998 *J. Am. Chem. Soc.* **120** 10629
[17] Pastor N 2005 *Biophys. J.* **88** 3262
[18] Mazur A K 2003 *J. Am. Chem. Soc.* **125** 7849
[19] Kornyshev A A and Leikin S 1998 *Proc. Natl Acad. Sci.* **95** 13579
[20] Kornyshev A A and Leikin S 1997 *J. Chem. Phys.* **107** 3656
[21] Kornyshev A A and Leikin S 1999 *Phys. Rev. Lett.* **82** 4138
[22] Wynveen A, Lee D J and Kornyshev A A 2005 *Eur. Phys. J.* E **16** 303
[23] Kornyshev A A, Lee D J, Leikin S and Wynveen A 2007 *Rev. Mod. Phys.* **79** 944
[24] Lindsay S M, Lee S A, Powell J W, Weidlich T, DeMarco C, Lewen G D, Tao N J and Rupprecht A 1988 *Biopolymers* **27** 1015–43
[25] Lavalle N, Lee S A and Rupprecht A 1990 *Biopolymers* **30** 877–87
[26] Lavalle N, Lee S A and Flox L S 1991 *Phys. Rev.* A **6** 3126–30
[27] Hasted J B 1973 *Water: A Comprehensive Treatise* ed F Franks (New York: Plenum)
[28] Liszi J and Ruff I 1985 *The Chemical Physics of Solvation* ed R R Dogonadze, E Kalman, A A Kornyshev and J Ulstrup (Amsterdam: Elsevier) chapter 4, p 119 Part A
[29] Hingerty B E, Ritchie R H, Ferell T L and Turner J E 1985 *Biopolymers* **24** 427
[30] Perepelytsya S M and Volkov S N 2004 *Ukr. J. Phys.* **49** 1072
[31] Rudd L 2007 *Thesis* to be published
[32] Bartenev V N, Golovamov E I, Kapitonova K A, Mokulski M A, Volkova L I and Skuratovskii I Y 1983 *J. Mol. Biol.* **169** 217
Lipanov A A, Alekseev D G, Bartenev V N, Volkova L I, Kapitonova K A and Skuratovskii I Y 1986 *Biofizika* **31** 336
Grosberg Yu, Nguyen T T and Shlovskii B I 2002 *Rev. Mod. Phys.* **74** 329
[33] LeBrett M and Zimm B H 1984 *Biopolymers* **23** 287
[34] Elsawy K M, Hodgson M K and Caves L S D 2005 *Nucleic Acids Res.* **33** 5749
[35] Banavali N K and Roux B 2005 *J. Am. Chem. Soc.* **127** 6866
[36] Olson W K and Sussman J L 1982 *J. Am. Chem. Soc.* **104** 270
[37] Brameld K A and Goddard W A III 1999 *J. Am. Chem. Soc.* **121** 985
[38] Arora K and Schlick T 2003 *Chem. Phys. Lett.* **378** 1
[39] Saenger W 1984 *Principles of Nucleic Acid Structure* (New York: Springer)
[40] Bartenev V N, Golovamov E I, Kapitonova K A, Mokulski M A, Volkova L I and Skuratovskii I Y 1983 *J. Mol. Biol.* **169** 217
[41] Shui X, McFail-Isom L, Hu G G and Dean Williams L 1998 *Biochemistry* **37** 8341–55
[42] Tereshko V, Minasov G and Egli M 1999 *J. Am. Chem. Soc.* **121** 3590
[43] McFail-Isom L, Sines C S and Dean Williams L 1998 *Curr. Opin. Struct. Biol.* **9** 298
[44] Malenkov G, Minchenkova L, Minyat E, Schyolkina A and Ivanov V 1975 *FEBS Lett.* **51** 1
[45] Cheatham T E III, Crowley M F, Fox T and Kollman P A 1997 *Proc. Natl Acad. Sci.* **94** 9626–30
[46] Lipanov A A, Alekseev D G, Bartenev V N, Volkova L I, Kapitonova K A and Skuratovskii I Y 1986 *Biofizika* **31** 336
Bartenev V N, Golovamov E I, Kapitonova K A, Mokulski M A, Volkova L I and Skuratovskii I Y 1983 *J. Mol. Biol.* **169** 217
[47] This was modelled similarly in Montoro J C G and Abascal J L F 1995 *J. Chem. Phys.* **103** 8273
[48] Harreis H M, Kornyshev A A, Likos C N, Löwen H and Sutmann G 2002 *Phys. Rev. Lett.* **89** 018303
[49] Langridge R, Wilson H R, Hooper C W, Wilkins M H F and Hamilton L D 1960 *J. Mol. Biol.* **2** 19
[50] Fuller W, Wilkins M H F, Wilson H R and Hamilton L D 1965 *J. Mol. Biol.* **12** 60
[51] Fuller W, Wilkins M H F, Wilson H R and Hamilton L D 1965 *J. Mol. Biol.* **12** 60
Langridge R, Wilson H R, Hooper C W, Wilkins M H F and Hamilton L D 1960 *J. Mol. Biol.* **2** 19
[52] Weidlich T, Lindsay S M and Rupprecht A 1998 *Phys. Rev. Lett.* **61** 14
[53] Ivanov V I, Minchenkova L E, Scholkina A K and Poletayev A I 1973 *Biopolymers* **12** 89
[54] Rupprecht A, Piskur J, Schultz J, Nordenskiold L, Song Z Y and Lahajnar G 1994 *Biopolymers* **34** 897
[55] Bartenev V N, Golovamov E I, Kapitonova K A, Mokulski M A, Volkova L I and Skuratovskii I Y 1983 *J. Mol. Biol.* **169** 217

[56] Lipanov A A, Alekseev D G, Bartenev V N, Volkova L I, Kapitonova K A and Skuratovskii I Y 1986 *Biofizika* **31** 336
[57] Bevan D R, Li L, Pedersen L G and Darden T A 2000 *Biophys. J.* **78** 668
[58] Good R H 1999 *Classical Electromagnetism* (Fort Worth: Saunders College Publishing)
[59] Kornyshev A A and Leikin S 2001 *Phys. Rev. Lett.* **86** 3666
[60] LeBrett M and Zimm B H 1984 *Biopolymers* **23** 287